

Full Length Research Paper

Development of a filter system using silver nanoparticles modified silica sand for drinking water disinfection

Margareth Msoka^{1,2}, Fortunatus Jacob² and Ally Mahadhy^{1*}

¹Department of Molecular Biology and Biotechnology, University of Dar es Salaam, Tanzania, P. O. Box 35179 Dar es salaam, Tanzania.

²Chemistry Department, University of Dar es Salaam, Tanzania, P. O. Box 35061 Dar es salaam, Tanzania.

Received 12 May, 2023; Accepted 27 June, 2023

This study presents a filter system for the removal of pathogenic microorganisms from potable water using silver nanoparticle-modified silica sand. While silica sand has potential applications in wastewater treatment, its effectiveness in microbial filtration falls short. Thus, there is a need for an environmentally friendly enhancement method. The silver nanoparticles were synthesized using *Commelina maculata* leaf extracts, and their diameter ranged from 50 to 80 nm. The Ag NPs were immobilized on silica sand, improving the modified sand's physicochemical properties. The filter system, composed of Ag NP-modified silica sand packed in a glass column, reliably removed 98% of the culturable *E. coli* population in water. The results suggest that the developed filter system has potential use in drinking water disinfection in remote rural areas. However, further cost analysis is required before scaling up for mass production and real-world use.

Key words; Silver nanoparticles, silica sand, *Commelina maculate*, microbial filtration, water treatment.

INTRODUCTION

Availability of safe drinking water is a major concern in Sub-Sahara African countries, with significant implications for public health and economic development. Water-borne diseases such as cholera, typhoid, and diarrhoea are prevalent, particularly in rural areas where families often rely on rivers and unprotected sources for domestic water needs. Despite efforts to promote household water treatment, only 18.2% of families treat their drinking water at home, contributing to the recurrence of water-borne infections (Sugumari et al., 2021). Additionally, poor construction and maintenance of water systems, damaged infrastructure, and a lack of hygiene and

sanitation knowledge in urban areas also lead to water contamination and associated health risks (Sadhana, 2016).

Silica sand is a common water filtration medium that has been used for over 150 years due to its inert and non-toxic nature. This inertness ensures that the sand does not introduce unwanted chemical into the water supply (Lavon and Bentury, 2015). However, the effectiveness of silica sand in removing contaminants from potable water is limited. Recent efforts to improve the effectiveness of silica sand filtration have focused on modifying the sand with chemically synthesized

*Corresponding author. E-mail: allymahadhy@yahoo.com. Tel: +255 656 133 034.

nanoparticles, which have shown promise in purifying drinking water (Munasir et al., 2020). However, conventional nanoparticle synthesis methods involve the use of toxic and hazardous chemicals, presenting significant environmental and health risks (Das et al., 2017).

Green synthesis of metallic nanoparticles using natural sources such as plants, animals, and microorganisms has emerged as a promising alternative approach (Das et al., 2017). Compared to chemical synthesis, these green synthesis methods can produce nanoparticles with lower toxicity and have fewer environmental impacts. In this study, a novel water treatment technology was developed, utilizing silica sand filters modified with non-toxic, green-synthesized nanoparticles derived from *Commelina maculata*. This plant, belonging to the *Commelinaceae* species, is readily available and is a small, perennial herbal plant mostly found in wet places. *Commelina maculata* offers a favourable environment for nanoparticle synthesis as it is free from toxic chemicals and provides natural capping agents (Shah et al., 2017). The extract of *Commelina maculata* has been shown to produce silver nanoparticles without toxicity, unlike their chemically synthesized counterparts (Eranga et al., 2017). This approach has the potential to offer an effective, efficient, and affordable means of achieving nanoparticles for water treatment and purification. Overall, the use of green-synthesized nanoparticles for water treatment is a promising approach that can potentially be employed in various fields, including environmental, biomedical, agricultural, and electronics.

MATERIALS AND METHODS

Materials

Fresh leaves of *Commelina maculata* and silica sand were obtained from two different locations in Tanzania: the vegetation at Mwalimu JK Nyerere campus of the University of Dar es Salaam (UDSM) at 6.77580S, 39.20900E and the seashore at Kigamboni in Dar es Salaam (6.82270S, 39.30240E) respectively. A glass column with a diameter of 1.5 cm and a length of 25 cm was fabricated at the UDSM Central Science Workshop. All chemicals utilized in the study were of analytical grade, procured from Sigma-Aldrich, and employed as received without undergoing any additional purification.

Methods

Preparation of plant extract

To prepare the plant extract, the method described in (Archana et al., 2021) was followed with minor modifications. Firstly, fresh leaves were thoroughly washed with distilled water to eliminate any dust particles and then air-dried at room temperature for one day. Next, 10 grams of the dried leaves were measured and ground into a smooth powder.

The powdered sample was then heated with 200 mL of sterile distilled water at 60°C for 5 min, and allowed to cool to room temperature. The sample was then filtered through a Chm No. F1001 filter paper, and the filtrate was collected. To remove any

heavy biomaterials present, the collected filtrate was centrifuged at 3000rpm for 15 min.

Biosynthesis of silver nanoparticles

To synthesize silver nanoparticles, a 1 mM solution of silver nitrate (AgNO₃) in 100 mL volume was prepared. 50 mL of an aqueous leaf extract of *Commelina maculata* species, which had been prepared beforehand using the method described in the (Archana et al., 2021) publication with minor adjustments, was added to the silver nitrate solution. The resulting mixture was then incubated in a dark and undisturbed environment at room temperature for 3 h, which led to the formation of silver nanoparticles.

Modification of silica sand with silver nanoparticles

To prepare the Ag NPs-modified silica sand, 100 grams of clay-free silica sand with average grain diameters of 420 µm, 3360 µm, and 4760 µm were measured individually and washed with water. Each sand sample was then soaked in 50 mL of Ag NPs suspension for 24 h, washed several times with distilled water, and oven-dried for 3 h. The dried sand samples were stored in a desiccator.

To set up the column, a glass column with a length of 25 cm and a diameter of 1.5 cm was clamped vertically. The column was then filled with the Ag NPs-modified silica sand. To prevent sand from leaking out of the lower end of the column, a 1 cm thick sterilized cotton wool was used to plug the column.

Determination of bacterial removal efficiency of the packed column

Two distinct operational modes were employed to examine the effectiveness of a column packed with Ag NPs-modified silica sand for microbiological water treatment. The first mode was a continuous flow system that utilized a peristaltic pump, and the second mode was a batch setup system driven by gravitational force. In each case, four separate beakers were filled with 100 mL of sterile water samples, and 1, 2, 4- and 10-mL volumes of nutrient broth containing 1.5×10^8 Cfu/mL bacteria (either *E. coli* or *S. typhi*) were transferred into each beaker. Subsequently, 2 mL of well-mixed contaminated water was extracted from each beaker to establish the initial bacterial concentration. The remaining contaminated water (about 98 mL) was then passed through the column either in continuous flow mode with a flow rate of 55.6 µL/s or in batch mode. After passing through the column, 2 mL of treated water was sampled from each beaker to determine the concentration of bacteria in the treated water.

To assess the effectiveness of the packed column, real water samples were collected from two different sources: stream water from the Academic Bridge at the Mwalimu J.K Nyerere campus of UDSM and tap water from the Chemistry laboratory at UDSM. The water samples were collected in 2 L sterilized polypropylene containers and their initial bacterial concentrations were determined. The bacterial concentration in the water samples was measured before and after treatment using two methods. The first method involved measuring the absorbance of the samples at a wavelength of 60 nm using spectrophotometry. The absorbance was directly proportional to the bacterial concentration in the sample. The second method involved determining the bacterial concentration in agar plates at 37°C for 24 h using the colony forming unit method. All experiments were conducted in triplicate.

The viability of bacteria (*E. coli* and *S. typhi*) in the water samples before and after treatment was also determined using an indicator dye called p-iodonitrotetrazolium (INT) at a concentration of 0.2 mg/mL (40 µL). The dye changes from colourless to pink



Figure 1. Aqueous Leaf Extract, Aqueous Synthesized C-Ag NPs and its Solid Synthesized C-Ag NPs.

Source: Authors

when in contact with living microorganisms.

RESULTS AND DISCUSSION

Biosynthesis of silver nanoparticles

A yellowish-brown colour solution was developed following mixing of silver ions with leaves extract (Figure 1). The successful synthesis of silver nanoparticles in a reaction mixture can be detected by the presence of a yellowish-brown colour. This colour is caused by the surface plasmon vibrations in the nanoparticles, as explained in a study by Protima et al. (2014). The reduction of silver ions by leaf extracts to form Ag NPs was confirmed by scanning the absorption maxima at the wavelength range from 200–700 nm using, SPECORD 210 PLUS UV-Vis spectrophotometer by Konrad Zuse Strasse1, Germany found at University of Dar es salaam Chemistry Department. The results showed a sharp surface plasmon band centred at 445 nm, which is a characteristic peak for silver nanoparticles. This peak falls within the range of 420-450 nm, which is typical for silver nanoparticles, as reported by Kero et al. (2017). In contrast, a control sample of leaf extract did not exhibit a peak at 445 nm, but rather showed a peak at 309 nm

(Figure 2b), indicating the absence of silver nanoparticles in this solution, as noted by Kero et al. (2017).

Characteristics of plant extract and synthesized silver nanoparticles

Chemical composition of commelina maculate (plant) extract and the reaction mixture

To identify the chemical composition of the *Commelina maculate* extract and the compound responsible for reducing, capping, and stabilizing the synthesized silver nanoparticles, FT-IR spectroscopy was used. The IR spectra were recorded by Perkin-Elmer 2000 FTIR spectrometer from America which found in UDSM Chemistry Department in the wavenumber range of 4000 cm^{-1} to 500 cm^{-1} . The FT-IR spectral results for (a) the *Commelina* extract and (b) the reaction mixture after the completion of the biosynthesis of Ag NPs are presented in Figure 3. Additionally, the technique was used to confirm the presence of silver nanoparticles.

The FTIR spectra presented in Figure 3 indicate that the *Commelina* extract contains molecules of different functional groups, such as hydroxyl and carbonyl groups. Specifically, Figure 3 (a) shows bands for the *Commelina*

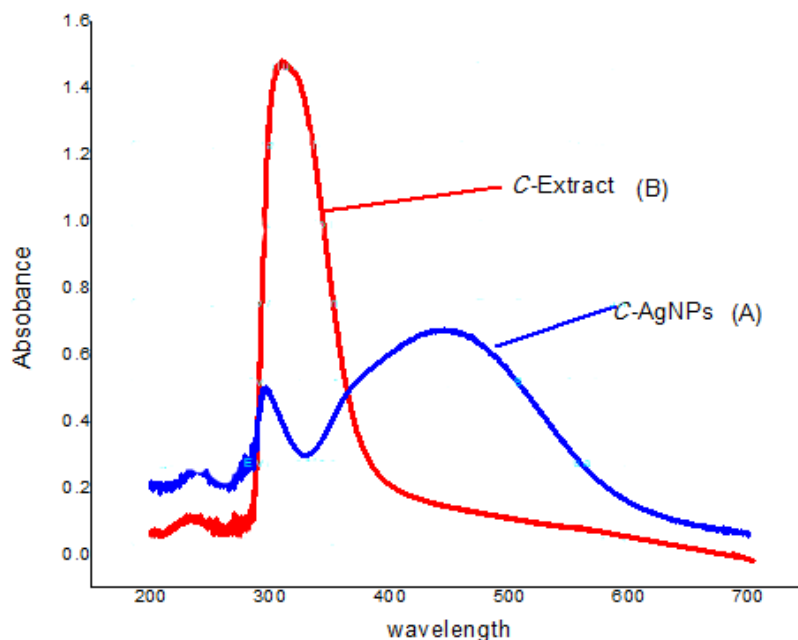


Figure 2. Showing UV-Vis Spectral Scans of the Reaction Mixture, *Commelina*-Ag NPs (A) and Control Sample, Plant Extract (B).
Source: Authors

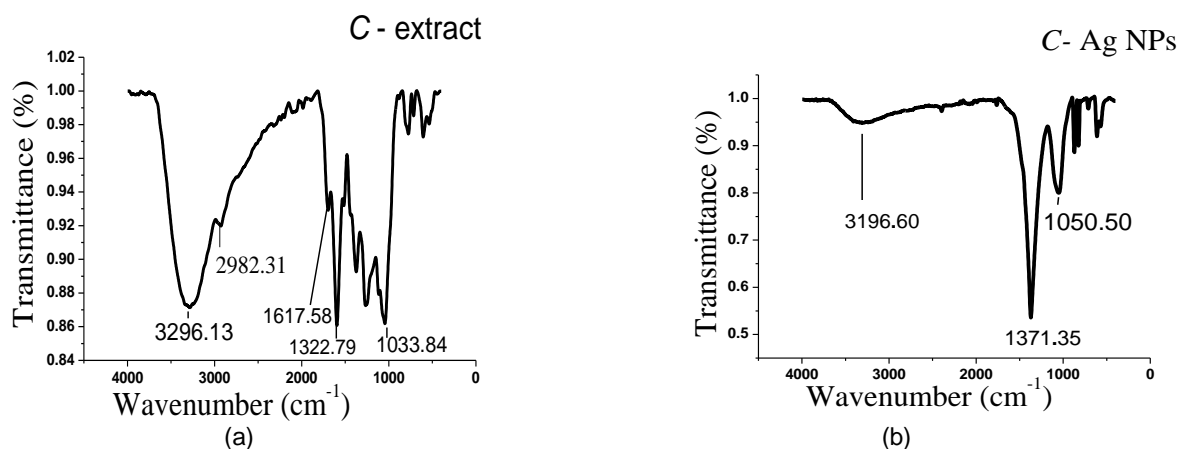


Figure 3. FTIR spectral scan of (a) *Commelina* extract and (b) biosynthesised Ag NPs.
Source: Authors

extract at 3296.13 cm^{-1} , 1617.58 cm^{-1} , 1322.79 cm^{-1} , and 1033.84 cm^{-1} , while Figure 3 (b) shows bands for the reaction mixture (C-Ag NPs) at 3201.60 cm^{-1} , 1371.35 cm^{-1} , and 1050.50 cm^{-1} .

The band at 3296.13 – 3201.60 cm^{-1} corresponds to a strong O-H stretching vibration, which indicates the very likely presence of phenols and alcohols (Petkovic, 2011). Furthermore, the peak at 1033.84 cm^{-1} in the *Commelina* extract and the peak at 1050.50 cm^{-1} in the C-Ag NPs sample are attributed to the O-H of, most likely, the

phenols, which are believed to aid in the reduction of Ag^+ into Ag^0 through the sharing of polyphenols, such as flavonoids and terpenoids.

The phenolic compounds such as lignin, phenolic acids, tannins, and stilbenes are responsible for the rapid reduction along with stabilizing and capping of silver ions into silver nanoparticles (Adhikari et al., 2022). On the other hand, the band at 1617.58 – 1322.79 cm^{-1} corresponds to amide group, which is a protein peptide bond (Yan et al., 2014). The absorption bands displayed

by the amides are usually due to N-H and C=O, C-C and to some extent from the C-N stretching vibrations. Accordingly, the peak observed at 1617.58 cm^{-1} in *Commelina* extract was designated for C-C and C-N stretching vibrations, indicating the presence of protein molecules. The peaks at 1322.79 cm^{-1} in *Commelina* extract and 1371.35 cm^{-1} in C-Ag NPs, were assigned for the proteins N-H vibration and N-H stretching vibrations, respectively.

These bonds usually present in the amide linkage of the proteins. In addition to the backbone amide modes, the bands at 1033.84 cm^{-1} and 1050.50 cm^{-1} regions, which are observed in *Commelina* extract and C-Ag NPs, respectively, contain absorption from many functional groups relevant to proteins and their side-chains (Huyan et al., 2015).

Therefore, these results suggest the presence of phenolic and protein molecules in both *Commelina* extract and C-Ag NPs samples. However, the latter was suggested to contain fewer phenolic and proteins molecules. This can be attributed to their involvement in the reduction and stabilization of synthesized Ag NPs, which is evidently by the slight variations in the O-H and N-H peaks patterns between the two samples and the disappearance of the band at 1617.58 cm^{-1} for C-C and C-N in C-Ag NPs sample.

Topographical and morphological characteristics of biosynthesised silver nanoparticles

AFM analysis

The topographical and morphological features of nanoparticles play a crucial role in determining their properties. These features include various factors such as size, shape, distribution, localization, agglomeration/ aggregation, surface morphology, surface area, and porosity of the nanoparticles, which collectively influence their behaviour (Stefanos et al., 2018). To examine the topographical and morphological characteristics of Ag NPs in this study, AFM was used. The synthesized silver nanoparticles were characterised by AFM digital instrument MMAFM-2 (Illinois, U.S.A) in the department of Physics at the University of Dar es salaam. Figure 4 illustrates the size and disparity of the particles.

The AFM analysis revealed that the biosynthesized silver nanoparticles (C-Ag NPs), produced using *Commelina maculate* extract, were spherical in shape and had a variable size range of 2 to 90 nm, with an average grain size of 51.36 nm. Despite being polydisperse, some agglomeration of C-Ag NPs was observed, which could be attributed to the magnetic properties of the individual silver particles or subunits. In some instances, particles larger than 100 nm were also observed, which might be due to the agglomeration caused by reaction parameters, such as the amount of reducing agent, as suggested by

Yasser et al. (2017). Similar findings have been reported in a study by Periasamy et al. (2022), where silver nanoparticles synthesized using *Hibiscus rosasinensis* leaf extract showed analogous results.

XRD analysis

The structural analysis of the synthesized Ag NPs was conducted by using X-ray diffractometer BTX SN 231(Kyoto, Japan) equipped with Co- $\text{K}\alpha$ radiation source to examine the crystalline nature of the biosynthesized C-Ag NPs. The X-ray diffraction (XRD) pattern was measured by drop coated films of Ag NPs of each sample on metal plate and employed with characteristic radiation in the range of $10\text{--}50^\circ$ at a scan rate of $0.05/\text{min}$ with the time constant of 2 s, Co- $\text{K}\alpha$ radiation and amplitude wave $k = 1.79\text{ \AA}$ working with a 30.5 kV voltage and 0.340 mA current. The full-width at half-maximum (FWHM) from five different peaks were used in Debye- Scherrer's equation to determine the average crystallite size of the nanoparticles (Raman et al., 2012).

The resulting XRD pattern (Figure 5) displayed six distinct reflections at specific angles: 22.74° , 26.32° , 37.58° , 44.40° , 46.46° , and 54.21° . These angles corresponded to Miller indices [hkl] (111), (109), (101), (204), (202), and (006) respectively, indicating a face-centred cubic configuration and a nanocrystalline structure for the particles. This finding aligns with the work of Khan et al. (2011). Importantly, no additional reflections beyond the Ag lattice were observed, suggesting that the biosynthesized C-Ag NPs are highly stable and unaffected by other molecules present in the *Commelina maculate* leaf extract.

Antibacterial activity

The disc diffusion method was employed to assess the antibacterial efficacy of the synthesized Ag NPs against two common waterborne pathogens: *E. coli* (ATCC 25922) and *Salmonella typhi* (*S. typhi*) (ATCC 19430). Erythromycin, a standard antibiotic, served as the positive control for the test pathogens. The results indicated that Ag NPs at a concentration of 40 mg/mL exhibited excellent antibacterial activity against both *E. coli* ($21.7\pm 0.2\text{ mm}$) and *S. typhi* ($19.3\pm 0.1\text{ mm}$), as evidenced by the zone of inhibition (ZOI) surrounding the discs. Figure 6 displays the ZOI of C-Ag NPs against each tested pathogen: (a) *E. coli* and (b) *S. typhi*. Table 1 shows antibacterial activity for synthesized Ag NPs and plant extract.

After conducting several dilutions of the synthesized Ag NPs, the minimum inhibitory concentration (MIC) was found to be 0.054062 mg/ml for *E. coli* and 0.05750 mg/ml for *S. typhi*. This finding aligns with the observation made by Espinosa et al. (2009) that smaller nanoparticles

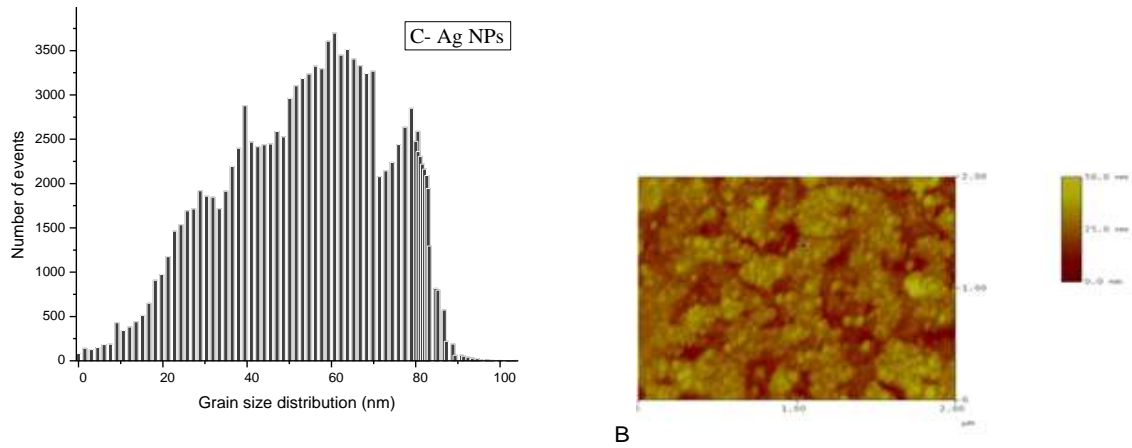


Figure 4. Particle Size Distribution of Ag NPs Synthesized by *Commelina* extract. Source: Authors

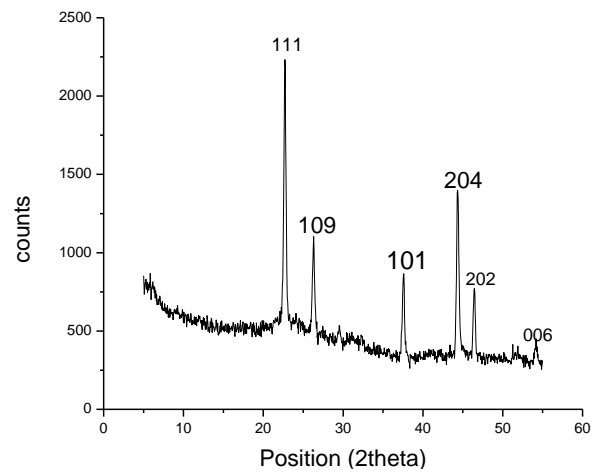


Figure 5. Depicting the X-ray diffraction pattern of crystalline nature of C-Ag NPs. Source: Authors

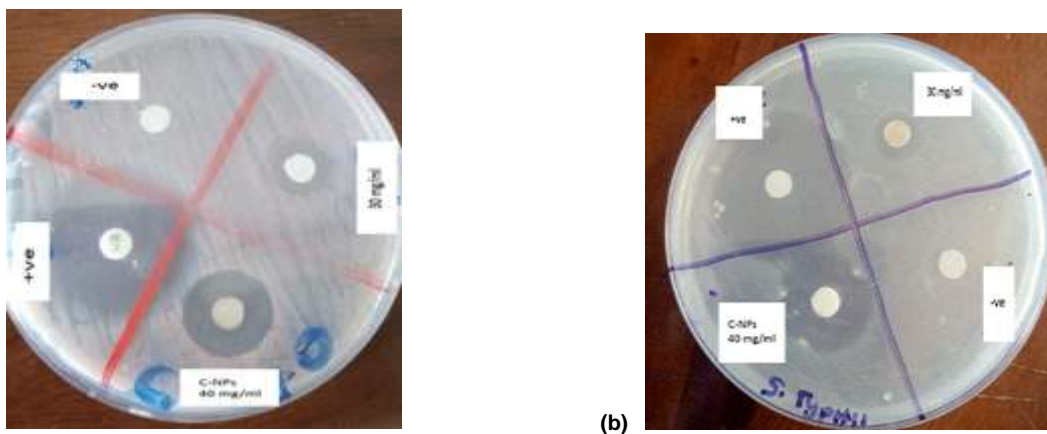
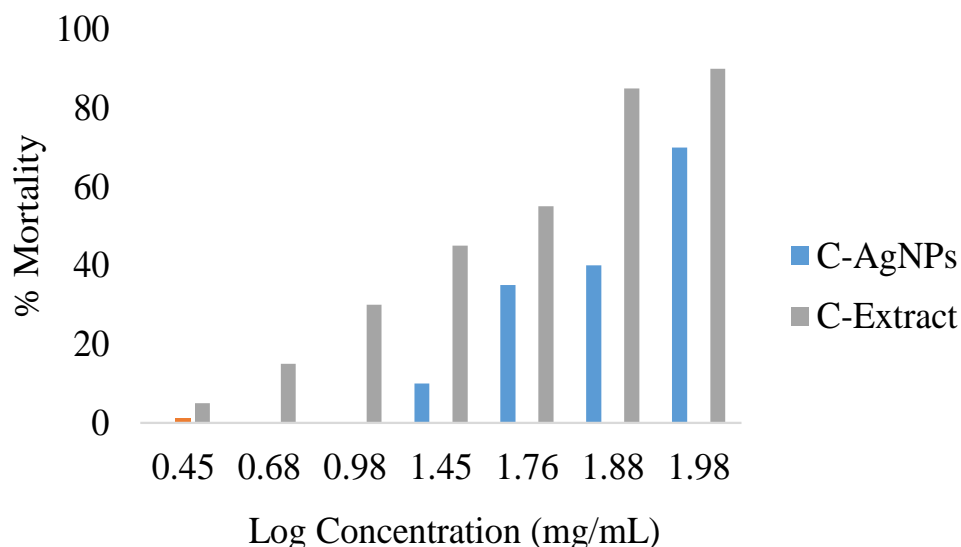


Figure 6. Antibacterial assay showing inhibition zone of 40 mg/ml C-Ag NPS against (a) *E. coli* and (b) *S. typhi*. Source: Authors

Table 1. Antibacterial Activity for Synthesized Ag NPs and plant extract.

Sample Type	Concentration (mg/mL)	Zone of inhibition (mm)	
		<i>E. coli</i>	<i>S. typhi</i>
C-Ag NPs	30	13±0.1	12±0.1
C-Ag NPs	40	21.7±0.2	19.3±0.1
C-extract (100%)	ND	0.0±0.0	0.0±0.0
Erythromycin (+ve control)	5×10 ⁻⁴	31.3±0.5	32.7±0.2
Sterile water (-ve control)	ND	0.0±0.0	0.0±0.0

Source: Authors

**Figure 7.** Showing Mortality Rate of Brine shrimp larvae Due Toxicity Effect of Plant Extract and Synthesized Ag NPs against Brine Shrimp larvae.

Source: Authors

have a lower MIC compared to larger ones. The synthesized Ag NPs exhibited an 80% minimum inhibition concentration at an optimal bacterial concentration of 10⁶ Cfu/mL, as reported by Retan et al. (2011). These results demonstrate the potential of *Commelina maculate* leaf extract as a valuable ingredient in nanotechnology for inhibiting various microorganisms and its application in water treatment.

Toxicity analysis

The *Commelina* extract and synthesized silver nanoparticles (C-Ag NPs) were studied for their toxicity using brine shrimp lethality bioassay (Figure 7).

The study found that both the *Commelina* extract and C-Ag NPs did not exhibit toxicity even at high concentrations. The LC50 values, which represent the concentration at which 50% of cells are killed, were 107.0 mg/ml and 44.0 mg/ml after 24 h for the extract and NPs,

respectively. A sample with an LC50 value above 0.1 mg/ml is considered non-toxic. These findings are consistent with previous studies such as Zan et al. (2020) and Zhou et al. (2018). Therefore, the study concludes that the *Commelina* extract contains biochemical compounds that can be used for the green synthesis of non-toxic Ag NPs, which have potential applications in disinfecting drinking water.

Application of synthesized Ag NPs in disinfection of water

Immobilization and characterization of Ag NPs on silica sand

The synthesized silver nanoparticles were immobilized on 3360 μm silica sand (Figure 8). Upon immobilization with Ag NPs, the colour of the silica sand changed from white to brown. Approximately 0.905 μg of Ag NPs was found



Figure 8. Presenting Natural Silica Sand Before and After Immobilization with Ag NPs.
Source: Authors

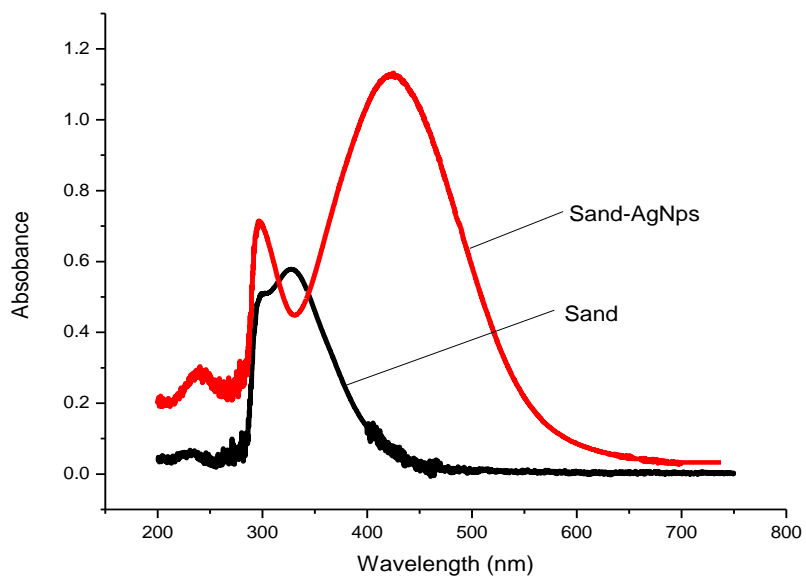


Figure 9. The UV-Vis absorption spectrum for Ag NPs-immobilized and non-immobilized silica sand.
Source: Authors

in every 100 g of immobilized silica sand. The presence of Ag NPs on the surface of the immobilized silica sand was analysed using UV-vis spectrophotometry. The results indicate that the silica sand contains silver nanoparticles, as evidenced by the UV-vis absorption peak remaining within the peak region at a wavelength of 438 nm, even after several washings with sterile water (Figure 9).

The structural features of Ag NPs-immobilized silica sand surface were characterized by AFM using an 80 μm scan range. The immobilized sand was scanned 2 mm to

the left and 10 mm to the right, as described by Rao et al. (2007). Surface texture parameters were calculated to evaluate the differences in the topographical surface of the silica sand before and after immobilization with Ag NPs. The roughness parameters (average roughness R_a , root mean square roughness R_q , maximum roughness R_y , and maximum profile peak height R_p , and roughness skewness R_{sk}) of the silica sand surface before and after immobilization with Ag NPs are presented in Table 2.

The results indicate a decrease in the roughness parameters of silica sand after immobilization with Ag

Table 2. Roughness parameters of silica sand before and after immobilization of Ag NPs.

Sample	R _a (nm)	R _q (nm)	R _y (nm)	R _p (nm)	R _{sk}
Sand before	134.2	161.2	400.8	248.1	423.4
Sand after	59.2	86.3	267.7	108.2	198.2

Source: Authors

NPs, suggesting the presence of a smoother surface. This smoother surface is likely a result of the even distribution of the immobilized Ag NPs on the silica sand. Similar observations have been reported in previous studies involving the immobilization of Ag NPs on silica sand or other surfaces (Alena et al., 2014).

Assessment of Ag NPs-Silica sand filter performance for bacteria removal in water

The performance of the silica sand-Ag NPs filter for bacteria removal in water was determined spectrophotometrically by measuring the optical density (OD) of water before and after passing through the column at 600 nm. Three different water samples were examined: (i) water contaminated with a known volume of bacterial culture, (ii) tap water, and (iii) stream water. It has been established that absorbance is directly proportional to the concentration of matter in the sample and is determined by the amount of light scattered in the water sample (Buchanan et al., 2017). Therefore, the higher the number of bacteria in the water sample, the higher the recorded absorbance on the spectrophotometer. Additionally, the presence of microorganisms in the water was also determined using an indicator called p-iodonitrotetrazolium (INT).

The study was conducted in two different experimental setups: batch and continuous flow modes. In the continuous flow mode, a silica sand filter without Ag NPs (non-modified silica sand filter) was used as a control setup.

The optical densities of all water samples were observed to decrease after treatment with Ag NPs-silica sand filters in both, batch and continuous flow modes, suggesting the effective removal of bacteria in the water samples. The same water samples, before and after treatment, was subjected to bacterial culturing; faecal coliforms were detected in all samples before treatment, but were not detected in treated ones. These results indicate that the entire treatment process is capable of removing bacteria, especially faecal coliforms which are the mostly causative of waterborne infection (Suvadhan, 2014). It has long been known that sand has been used as a filter to purify drinking water in many industry (Saad et al., 2016), and silica sand has been used to purify water as it has ability to trap microorganism (Rafael, 1992).

However, the contribution of Ag NPs in bacterial removal from water sample is clearly demonstrated in this study by the observed smaller change in optical density of water samples treated with unmodified (control) silica sand filter compared to Ag NPs-modified silica sand filter. For instance, the optical density decreases of 6 and 97% were recorded for stream water treated with control and Ag NPs-modified silica sand filters, respectively. In other words, the column packed with Ag NPs-modified silica sand has more than 10 times bacterial removal capacity than the one packed with unmodified silica sand (control).

The contribution bacterial removal effect of Ag NPs can be attributed to the adsorption affinity of the reduced silver towards the bacterial cell wall (Shkodenko et al., 2020). Either, the presence of viable bacteria in the same water samples was determined by using an indicator dye, p-iodonitrotetrazolium (INT). All water samples changed the colour, from colourless to pink, upon addition of INT dye. However, no colour change was observed in any water sample after treatments.

Silver nanoparticles are well known to have the ability of penetrating bacterial cell walls, destroying the cell membranes and even resulting in cell death. Their efficacy is contributed by both, their nanoscale size nature and large surface area to volume ration properties (Linlin et al., 2017). Moreover, continuous flow showed to be more effective (97%) in bacterial removal from tap/stream water samples than the batch mode (93%), This is because the water in continuously filter being fluffed and swirl in an upflow design since it has more contact with the filter media thus produce better results (Brastad et al., 2013). While the use of batch mode depends on gravitational force, water flow may push through the device without significant interaction with the media (Linlin et al., 2017). Furthermore, drinking water is not expected to contain detectable amounts of Ag+/Ag NPs; if found, it is considered to be contamination (Gupta et al., 2019).

Leakage/leaching of Ag NPs in treated water were also determined. The amount of Ag NPs in treated water was found to be 3.87 femtogram (fg)/L of the collected water sample after treatment. However, no further leaching was observed after passing the first 100 ml, and the column retains almost all Ag NPs on the surface (> 99.95). This explains that, Ag NPs coated/immobilized on silica sand are stable and firmly adsorbed on the sand surface, allowing them to work with high efficiency and at minimum cost compared to other commonly used methods such as

ozonation, which require vast amounts of energy and capital (Naicker et al., 2023). The World Health Organisation (WHO) recommends that the maximum allowable concentration of silver in drinking is 0.1 mg/L (WHO, 2017), which is extremely higher, about 10^{11} , than the one recorded in this study. Typically, silver concentrations in surface water and groundwater are observed to be below 2 µg/L (ATSDR, 1990). On average, the concentrations of silver in these natural water sources have been documented to range from 0.2 to 0.3 µg/L (UEPA, 1980). Furthermore, neither faecal coliforms nor *E. coli* was detected in the filtered water by developed column. The absence of both faecal coliforms and *E. coli* in the filtered water, despite their detection in the original water sample, demonstrates the efficacy of the entire treatment process in removing bacteria. This is particularly significant for faecal coliforms, which are commonly associated with waterborne infections and pose a significant health risk (Forstinus et al., 2016).

Conclusion

Overall, this study highlights the potential of using green synthesis methods to produce bio-functional and non-toxic Ag NPs, which can be used for disinfection of drinking water. The use of locally available plants, such as *Commelina maculate*, makes the process more sustainable and cost-effective. The Ag NPs-modified silica sand filter demonstrated a high bacterial removal efficiency of 98% while maintaining minimal Ag NPs leakage. However, further studies are required to assess the long-term stability and effectiveness of the filter under different water treatment conditions. Overall, this approach holds promise as a safe and effective method for providing access to clean drinking water in regions with limited resources

CONFLICT OF INTERESTS

The authors have not declared any conflict of interests.

REFERENCES

- Archana KM, Rajagopal R, Krishnaswamy VG, Aishwarya S (2021). Application of Green Synthesised Copper Iodide Particle on Cotton Fabric-Protective Face Mask Material against COVID-19 Pandemic. *Journal of Materials Research and Technology* 15:2102-2116.
- Adhikari A, Chhetri K, Acharya D, Pant B, Adhikari AD (2022). Green synthesis of Iron Oxide nanoparticles using Psidium Gwajava Leaves Extract for Degradation of Organic dye and Antimicrobial Application. *Catalysts* 12(10):1188-1191.
- Agency for Toxic Substances and Disease Registry (ATSDR) (1990). *Toxicological Profile for Silver*.
- Alena R, Zdnka N, Zdenk K (2004). Immobilization of Silver Nanoparticles on Polyethylene Terephthalate. *Journal of Nanoscale Research* 10:305-315.
- Brastad KS, He Z (2013). Water Softening Using Microbial Desalination Cell Technology. *Desalination* 309:32-37.
- Buchanan CM, Wood RL, Hoj TR, Alizadeh M, Bledsoe CG, Wood ME, McClellan DS, Blanco R, Hickey CL, Ravsten TV, Hussein GA (2017). Rapid Separation of Very Low Concentration of Bacteria from Blood. *Journal of Microbiological Methods* 139:48-53.
- Das RK, Pachapur VL, Lonappan L, Naghdi M, Pulicharla R, Maiti S, Cledon M, Dalila LM, Sarma SJ, Brar SK (2017). Biological synthesis of metallic nanoparticles: plants, animals and microbial aspects. *Nanotechnology for Environmental Engineering* 2:1-21.
- Eranga R, Chanica J and Dulashin R (2017). Honey Mediated Green Synthesis of Nanoparticles. *Journal of Nanomaterials* 3:118-139.
- Forstinus N, Ikechukwu N, Emenike M, Christiana A (2016). Water and waterborne diseases: A review. *International Journal of Tropical Disease and Health* 12(4):1-4.
- Gupta S, Khare D, Mishra N, Sharma AK (2019). Waste water parameters and its Imperishable Augmentation.
- Kero J, Sandeep B, Sudhakar P (2017). Synthesis, Characterization, and Evaluation of the Antibacterial Activity of *Allophylus serratus* Leaf and Leaf Derived Callus Extracts Mediated Silver Nanoparticles. *Journal of Nanomaterials*.
- Khan Z, Hussain JI, Kumar S, Hashmi AA, Malik MA (2011). Silver Nanoparticles Green Route Stability and Effect of Additives. *Journal of Biomaterials and Nanobiotechnology* 2(4):390.
- Lavon O, Bentury Y (2015). Silica Gel: Non-Toxic Ingestion with Epidemiologic and Economic Implications. *The Israel Medical Association Journal* 17(10):604-606.
- Linlin W, Chen H, Longquan S (2017). The antimicrobial activity of nanoparticles: present situation and prospects for the future. *International Journal of Nanomedicine* 7:1227-1249.
- Munasir M, Hidayat N, Kusumawati DH, Putri NP, Taufiq A, Sunaryono S (2020). Amorphous-SiO₂ nanoparticles for water treatment materials. In *AIP Conference Proceedings* 2251(1) AIP Publishing.
- Naicker KI, Kaweesa P, Daramola MO, Iwarere SA (2023). Non-Thermal Plasma Review: Assessment and Improvement of Feasibility as a Retrofitted Technology in Tertiary Wastewater Purification. *Journal of Applied Sciences* 13(10):6243.
- Periasamy S, Jegadeesan U, Sundaramoorthi K, Rajeswari T, Tokala VN, Bhattacharya S, Muthusamy S, Sankoh M, Nellore MK (2022). Comparative analysis of synthesis and characterization of silver nanoparticles extracted using leaf, flower, and bark of *hibiscus rosasinensis* and examine its antimicrobial activity. *Journal of Nanomaterials* 10:812-854.
- Petkovic M (2011). O–H stretch in phenol and its hydrogen-bonded complexes: band position and relaxation pathways. *The Journal of Physical Chemistry* 116(1):364-371.
- Protima R, Erwa R, Stanislav F and Mangala P (2014). Silver nanoparticles: Synthesis and Application. *Journal of Advanced Research* 4:2-9.
- Rafael G (1992). Ripening of Silica Sand Used for Filtration. *Water Research* 1:10-19.
- Raman N, Sudharsan S, Veerakumar V, Pravin N, Vithiya K (2012). *Pithecellobium dulce* mediated extra-cellular green synthesis of larvicidal silver nanoparticles. *Spectrochimica Acta Part A: Molecular and Biomolecular Spectroscopy* 96:1031-1037.
- Rao A, Schoenenberger M, Gnecco E, Glatzel T, Meyer E, Brändlin D, Scandella L (2007). Characterization of nanoparticles using atomic force microscopy. In *Journal of Physics: Conference Series* 61(1):971.
- Retan D, Gang S, Nath SS (2011). Preparation and Antibacterial Activity of Silver Nanoparticles. *Journal of Biomaterials and Nanobiotechnology* 2(4):472.
- Saad FNM, Jamil MN, Odli ZSM, Izhar TNT (2016). Study on Modification Towards Water Quality of Wet Market Waste Water. *MATEC Web of Conferences* 78:101104.
- Sadhana C (2016). Traditional Water Purification Methods used in Rural area. *Department Energy Environmental* 8:12-33.
- Shah MD, D'souza UJ, Iqbal M (2017). The potential protective effect of *Commelina nudiflora* L. against carbon tetrachloride (CCl₄)-induced hepatotoxicity in rats, mediated by suppression of oxidative stress and inflammation. *Environmental Health and Preventive Medicine* 22(1):1-9.
- Shkodenko L, Kassirov I, Koshel E (2020). Metal Oxide Nanoparticles Against Bacteria Biofilm: Perspectives and Limitations. *Microorganisms* 8(10):1545.

- Stefanos M, Rogers M, Nguyen T (2018). Characterization Techniques for Nanoparticles: Comparison and Complementary upon Studying Nanoparticles Properties. *Journal of Nanoscale* 4:12871-12934.
- Sugumari V, Krisha S, Khangton S (2021). Development in Magnetic Nanoparticles and Nano-composite for Wastewater Treatment. *Journal of Jece* 7:116-132.
- Suvadhan K (2014). Nanotechnology for Water Treatment. *International Journal of Environmental Analytical Chemistry* 4:41-72.
- United States Environmental Protection Agency (UEPA) (1980). Ambient Water Quality Criteria for Silver. Report Number. EPA 440/5-80-071. Environmental Protection Agency, USA.
- World Health Organization (WHO) (2017). Drinking Water quality 4th Edition. Incorporating the 1st Addendum 1:1-10.
- Yan J, Yang X, Ying Q (2014). Poly-Amidoamine Structures Characterization: Amide Resonance Structure Imidic Acid and Tertiary Ammonium. *Journal of Advanced Research* 1:16-90.
- Yasser Z, Kyong Y, David H (2017). Influence of Nanoparticles aggregation/ Agglomeration on the Interfacial and Tensile Properties of Nanocomposite. *Journal of Computer Part B. Engineering* 4:10-12.
- Zan K, Chen XQ, Zhao MB, Jiang Y, Tu PF (2020). Cytotoxic sesquiterpene lactones from *Artemisia myriantha*. *Phytochemistry Letters* 37:33-36.
- Zhou X, Friedmann KS, Lyrmann H, Zhou Y, Schoppmeyer R, Knörck A, Mang S, Hoxha C, Angenendt A, Backes CS, Mangerich C (2018). A Calcium Optimum for Cytotoxic T Lymphocyte and natural Killer Cell Cytotoxicity. *The Journal of physiology* 596(14):2681-2698.